Shear Strength of SFRC Beams without Coarse Aggregate using Finite Element Analysis with Bond-Slip

D. Christianto[1], Tavio[2]*, M. R. Irianto[3]

Abstract–*The numerical evaluation of the shear strength of steel-fiber reinforced concrete (SFRC) beams without coarse aggregate using data from previous research has been performed in MIDAS FEA. The SFRC beams are modeled by using the total strain crack model with Thorenfeldt for compression behavior and brittle tension behavior. Modified bond stress-slip functions proposed by fib have been used to model the bond between concrete and reinforcement. From the finite element analysis, the cracking pattern and the maximum load at failure of SFRC beams without coarse aggregate have been similar to the test results. As the longitudinal reinforcement ratio increases above 3%, the finite element analysis starts to give overestimated maximum load. The highest ratio of maximum load from analysis and test results equal to 136% has been obtained from 7.82% reinforcement. It is also observed that the influence of longitudinal reinforcement ratio on the shear strength of SFRC without coarse aggregate is lower compared to normal-strength concrete predicted by ACI 318-19. Further studies on bond stress-slip relationship of SFRC without coarse aggregate are needed.*

Keywords*: bond-slip, coarse aggregate, concrete shear strength, MIDAS FEA, steel fiber*

Nomenclatures

ACI = American Concrete Institute;
A_s = longitudinal bars sectional area (mm^2);
a = shear span (mm);
b = beam width (mm);
C_1 = normalized shear stress coefficient;
C_2 = exponent factor for ρ;
d = beam effective depth (mm);
d_b = longitudinal bar diameter (mm);
FEA = finite element analysis;
fib = *fédération de internationale du béton*;
f'_c = concrete compressive strength (MPa);
f_{cm} = mean concrete compressive strength (MPa);
f_y = reinforcement yield strength (MPa);
M_n = nominal bending capacity (kNm);
P = maximum concentrated load (kN);
P_{FEA} = maximum load from FEA (kN);
P_M = maximum load based on the moment capacity of the beam (kN);
P_{TEST} = maximum load from the test (kN);
P_V = maximum load based on ACI 318-19 concrete shear capacity (kN);
SFRC = steel fiber reinforced concrete;
s = bond slip (mm);
s_1 = bond slip at the beginning of $\tau_{b,max}$ (mm);
s_2 = bond slip at the end of $\tau_{b,max}$ (mm);
s_3 = bond slip at the beginning of τ_f (mm);
s_4 = bond slip at the end of τ_f (mm);
V_c = concrete nominal shear capacity (kN);
v_{norm} = normalized shear stress;
λ = lightweight concrete modification factor;
λ_s = size effect factor according to ACI 318-19;
τ_b = bond stress (MPa);
$\tau_{b,max}$ = bond strength, maximum bond stress (MPa);
τ_f = residual bond stress (MPa);
α = exponent factor for bond stress;
ρ = longitudinal reinforcement ratio.

I. Introduction

Advances in construction technology have made it possible to build very tall concrete buildings. As the building height increases, the concrete strength needs to be increased in order to limit column dimensions to a reasonable proportion. There are many innovative solutions to increase concrete strength, for example, by adding steel fibers [1]-[3], using fiber bars and sheets [4]-[9], using a new type of transverse reinforcement [10], using waste materials [11]-[12], and/or removing coarse aggregate [13]-[18]. The removal of coarse aggregate is carried out to increase homogeneity and eliminate weak points due to the presence of coarse aggregate in the concrete mix.

In seismic-prone areas, the building should perform well in the event of an earthquake. The building should be able to dissipate energy without collapsing through the detailing of concrete elements, using a seismic damping device, or other means [19]-[20]. Especially in concrete buildings, the concrete weight gives a significant contribution to the overall weight of the structure, which further increases the seismic force that must be endured. Thus, high-strength concrete with lower density than normal-weight concrete, such as concrete without coarse aggregate, should be considered as an alternative material,

Manuscript received and revised xx 2010, accepted xx 2010

especially in high seismic areas.

All concrete structural members shall have adequate strength against flexure, shear, axial, and torsion. The strength is obtained from various research and/or building codes. Currently, building codes, such as ACI 318-19, are based on research on conventional concrete with coarse aggregate. Therefore, using such building codes to design steel fiber reinforced concrete (SFRC) members with or without coarse aggregate might lead to unsafe design or overly conservative design. The behavior of this type of concrete should be first understood and verified through extensive research before it can be used in construction.

One particular interest in the behavior of the reinforced concrete element is its behavior in shear failure [21]. This failure has a brittle nature and it is very undesirable in seismic-resistant buildings. In high-strength concrete without coarse aggregate, the concrete becomes even more brittle. Despite its brittle nature, the shear behavior of concrete is not yet completely understood due to its complexity. According to Joint ACI-ASCE Committee 445 [22], the shear in concrete is transferred by shear stress in the uncracked concrete compression zone, aggregate interlock, dowel and arch actions, and residual tensile stress.

Various studies have been carried out to investigate the behavior of SFRC and reinforced concrete without coarse aggregate, especially their shear behavior. The higher the steel fiber content in the concrete is, the higher the shear strength of the concrete is. However, in order to ensure the workability of the concrete, the steel fiber content should be limited to 0.3% of the total volume [1].

Christianto et al. [13] have shown that there is an 82.82% increase in the shear strength of concrete beams without coarse aggregate when the longitudinal reinforcement ratio is increased from minimum to maximum ratio. When 0.1% steel fibers have been added to the concrete mix, the increase in concrete shear strength reaches an even higher value of 108% [14]. It is also observed that the shear capacity of concrete beams without coarse aggregate is lower than the shear capacity of normal concrete (with coarse aggregate) [13]-[14]. Further studies have shown that the influence of longitudinal reinforcement ratio (dowel action) on the shear strength of concrete beams without coarse aggregate is lower than on concrete beams with coarse aggregate [15].

Similar to normal concrete, the shear strength of SFRC also increases when the shear span to depth ratio decreases to less than about 2.5, indicating deep beam behavior [16]. The increase in shear strength is caused by arch action, transferring the load as shear and compression directly to the supports. Christianto et al. [17] have also shown that there is a size effect in the shear strength of concrete beams without coarse aggregate. Further studies have shown that the size effect behavior agrees well with Bažant's size effect law [18].

As of now, numerical evaluation of the shear capacity of concrete without coarse aggregate is very limited. Currently, many commercial programs can perform numerical evaluation, such as finite element analysis (FEA), with relative ease. The availability of many FEA programs makes it relatively easy to verify the experimental results with FEA predictions. In developing the FEA model, modeling the basic material behavior is very important to predict the behavior of the structure.

Generally, concrete cracks can be modeled using a discrete crack model (discrete elements at crack locations) or using a smeared crack model (cracks are evenly scattered over wide surfaces) [23]. The smeared crack model can be further divided into the decomposed-strain model (total strain calculated as material strain and crack strain) and the total strain model. Total strain models are preferred due to their simplicity in defining the nonlinear behavior of material [23]. In the total strain crack model, concrete is modeled using two stress-strain relationships, one for tensile behavior and one for compressive behavior.

There are several compression models for concrete.

One of the models is suggested by Thorenfeldt, shown in Fig. 1. When concrete is compressed beyond its ultimate compressive strength, the concrete does not fail immediately. As concrete strain (deformation) increases beyond the strain corresponding to the maximum compressive strength, the load-carrying capacity of concrete will gradually decrease. This behavior is an indication of the ductility of concrete at the material level [4].

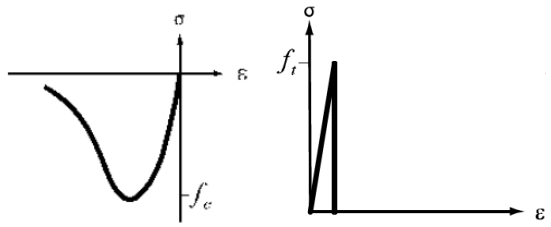

Fig. 1. Thorenfeldt compression model dan brittle tension model [23]

The tensile behavior of concrete can be modeled using the brittle model, as can be seen in Fig. 1. The stress-strain curve below the maximum tensile strength (peak point) of concrete is linear elastic. Beyond that peak point, the stress drops to zero indicating no softening behavior [4].

Another important behavior in developing a finite element model for concrete is bond slip. In reinforced concrete, flexural compressive forces are resisted by concrete and the flexural tensile forces are resisted by reinforcement [24]. For this mechanism to exist, a force transfer between concrete and reinforcement, which is called bond stress, should exist. In engineering practice, bond slip is typically neglected in the nonlinear analysis of reinforced concrete structures. Jendele and Cervenka [25] have shown that bond modeling always improves analysis results and it is important in obtaining the correct ultimate load-carrying capacity.

The bond between concrete and reinforcement is influenced by structural characteristics, reinforcement bar properties, and concrete properties [26]. Bond strength increases with increasing concrete cover, reinforcement

bar spacing, splice and development length, and concrete compressive and tensile strength. Reinforcement bar geometry (deformed or smooth) and its casting position also affect bond strength. The presence of steel fiber and transverse reinforcement also increases bond strength.

In order to model bonds, the simplified bond stress-slip function summarized by fib [27], as shown in Fig. 2, can be used. In Fig. 2, curve (I) applies to the steel bar in the elastic range, and curve (II) applies to the steel bar in the plastic range. For bar slip (s) not greater than s_1, bond stress (τ_b) can be expressed by the following relationship:

$$\tau_b = \tau_{b,max}\left(\frac{s}{s_1}\right)^{\alpha} \quad (1)$$

From the evaluation of test data [27] of normal-strength and high-strength concrete in "good" bond conditions, bond strength ($\tau_{b,max}$) can be taken as

$$\tau_{b,max} = 0.45 f_{cm} \quad (2)$$

For the "other" bond condition, bond strength from Eq. (2) should be reduced by 50%. Other parameters needed to construct the bond stress-slip function are tabulated in Table I.

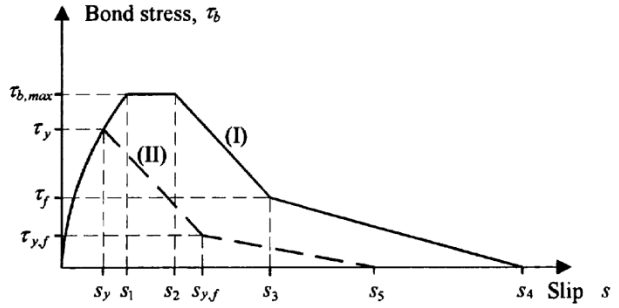

Fig. 2. Simplified bond stress-slip function [27]

TABLE I
SIMPLIFIED BOND STRESS SLIP PARAMETERS [27]

Parameters	Normal-Strength Concrete	High-Strength Concrete
s_1	1.0 mm	0.5 mm
s_2	3.0 mm	1.5 mm
s_3	Clear rib spacing	Clear rib spacing
s_4	3(rib spacing)	3(rib spacing)
α	0.4	0.3
τ_f	$0.4\tau_{b,max}$	$0.4\tau_{b,max}$

It should be noted that the bond stress-slip relationship in Fig. 2 is based on the testing of deformed (ribbed) bars in well-confined concrete. Thus, the relationship in Fig. 2 cannot be readily used for plain bars. For normal-strength concrete, the bond strength of plain bars is about 12% of the bond strength of ribbed bars in confined concrete [28]. Xing et al. [29] have shown that the bond strength ratio of plain (smooth) bars to deformed bars is about 18.3%.

In this paper, the SFRC beam specimens will be evaluated using finite element analysis in MIDAS FEA. This paper starts with a review of previous research on the shear behavior of concrete without coarse aggregate and concrete modeling in finite element analysis. The explanation of the concrete specimen's composition, experimental test methods, and analytical model in MIDAS FEA will be presented in the next section. The results are presented in the form of tables and graphs, followed by a discussion.

II. Methods

Experimental data of SFRC without coarse aggregate are obtained from Christianto et al. [14]. The SFRC specimens used have been made from water, ordinary portland cement, silica fume, sand from sieve No. 30 (0.6 mm), and No. 50 (0.3 mm), and marble powder from sieve No. 200 (0.075 mm), superplasticizer, and steel fiber. The material composition is listed in Table II.

TABLE II
SFRC SPECIMEN'S MATERIAL COMPOSITION [14]

Material	Density (kg/m^3)	Ratio
Cement	3150	1
Sand	2617.8	1.1
Silica fume	2200	0.2
Water	1000	0.18
Marble powder	2563	0.1
Superplasticizer	1150	0.025
Steel fiber	7850	0.001

The dimensions of SFRC beam specimens tested by Christianto et al. [14] are given in Fig. 3. The dimensions for all beam specimens are 70 mm × 125 mm × 1100 mm. Stirrups have not been used in the SFRC beam specimens. Two longitudinal smooth bars with a diameter (d_b) varied from 6 mm to 19 mm have been used in the SFRC beam specimens. The test results from Christianto et al. [14] are given in Table III.

TABLE III
TEST RESULTS OF SFRC SPECIMENS [14]

Beam ID	d_b (mm)	f'_c (MPa)	P_{TEST} (kN)	Failure type
E11	6	78.57	15.12	Flexure
E12	6	81.04	14.73	Flexure
E21	8	65.54	16.06	Flexure-Shear
E22	8	61.02	17.37	Flexure-Shear
E31	10	54.73	17.31	Shear
E32	10	69.25	23.13	Shear
E41	12	72.61	21.05	Shear
E42	12	58.18	23.81	Shear
E51	16	72.68	29.73	Shear
E52	16	74.40	29.94	Shear
E61	19	78.57	29.11	Shear
E62	19	70.65	27.70	Shear

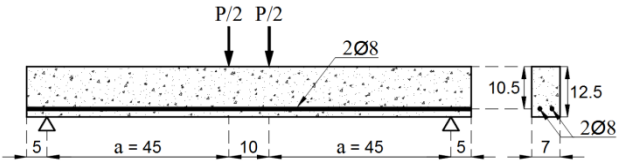

Fig. 3. SFRC beam specimens [14]

All finite element models of SFRC beam specimens are modeled in MIDAS FEA. The beams are modeled by using a 3D element. The total strain crack model is used to model concrete properties with compressive behavior defined by the Thorenfeldt model and tensile behavior defined by the brittle model. The steel reinforcement bars

are modeled by using the von mises model. The meshing results of the beam are shown in Fig. 4.

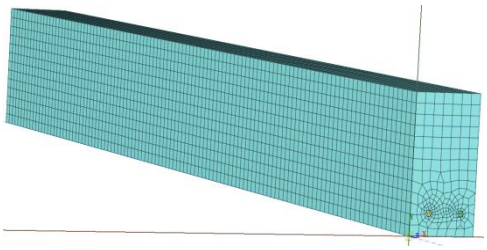

Fig. 4. Beam model with the meshing result

The bond between concrete and reinforcement is modeled using a 2D interface element with interface nonlinearities option taken as bond slip. Since the SFRC beam specimens use plain reinforcement bars, it is assumed that the bond stress-strain relationship from Fig. 2 for high-strength concrete can be used with a reduced bond stress value. In this research, it is assumed that the bond stress of plain bars can be taken as 18% of deformed bars. It is also assumed that f_{cm} is equal to f'_c. The bond stress-slip function parameters used in the models are given in Table IV. For all beams, s_1 = 0.5 mm, s_2 = 1.5 mm, and α = 0.3.

TABLE IV
BOND STRESS-SLIP PARAMETER

Beam ID	s_3 (mm)	s_4 (mm)	$\tau_{b,max}$ (MPa)	τ_f (MPa)
E11	4.2	12.6	35.36	14.14
E12	4.2	12.6	36.47	14.59
E21	6.3	18.9	29.49	11.80
E22	6.3	18.9	27.46	10.98
E31	7.0	21.0	24.63	9.85
E32	7.0	21.0	31.16	12.47
E41	8.4	25.2	32.67	13.07
E42	8.4	25.2	26.18	10.47
E51	11.2	33.6	32.71	13.08
E52	11.2	33.6	33.48	13.39
E61	13.3	39.9	35.36	14.14
E62	13.3	39.9	31.79	12.72

The beam's boundary conditions are modeled as hinge support and roll support (similar to simple beam support in 2D analysis). The concrete's self-weight is distributed to all the elements based on the concrete density. A pair of concentrated loads, with the value of $P/2$ each (Fig. 3), are uniformly distributed over the width of the beam.

Manual calculations of the maximum load based on moment capacity (P_M) and concrete shear capacity (P_V) are also performed for comparison. By using the strain compatibility method from ACI 318-19 [30], the nominal moment capacity (M_n) of the beam can be taken as

$$M_n = A_s f_y \left(d - \frac{A_s f_y}{1.7 f'_c b} \right) \quad (3)$$

For concrete beams without transverse reinforcement and axial load, ACI 318-19 [30] gives concrete shear strength (V_c) as

$$V_c = 0.66 \lambda_s \lambda (\rho)^{1/3} (f'_c)^{1/2} bd \leq 0.42 \lambda (f'_c)^{1/2} bd \quad (4)$$

with ρ taken as $A_s/(bd)$. For $d \leq 250$ mm, the size effect factor (λ_s) is equal to 1. ACI 318-19 limits f'_c to 70 MPa for the determination of V_c due to a lack of test data [30]. In this research, this limitation is ignored. For concrete without coarse aggregate, λ can be taken as 1 [17].

III. Results and Discussions

The cracking pattern at failure obtained from the experiment [14] and finite element analysis for all SFRC beam specimens are given in Fig. 5 to Fig. 16. It can be seen that the cracking pattern from MIDAS FEA is similar to the cracking pattern from the experiment.

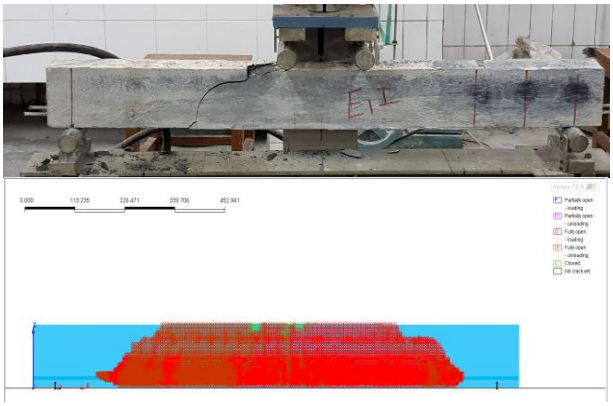

Fig. 5. Failure and Cracking Pattern of Beam E11

Fig. 6. Failure and Cracking Pattern of Beam E12

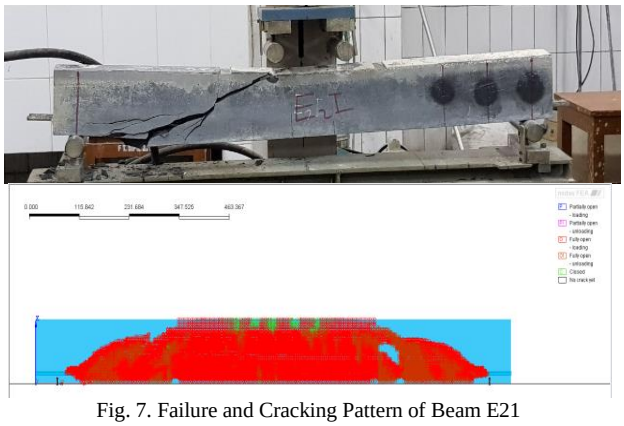

Fig. 7. Failure and Cracking Pattern of Beam E21

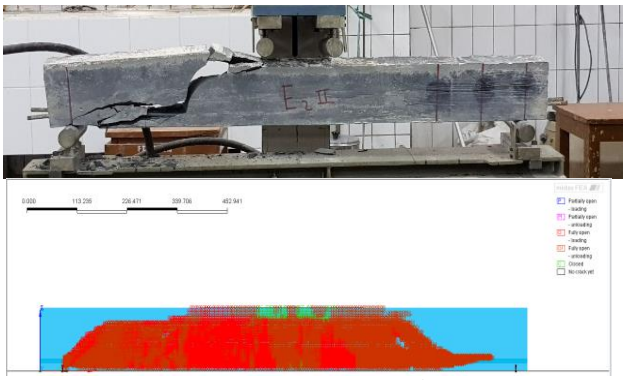

Fig. 8. Failure and Cracking Pattern of Beam E22

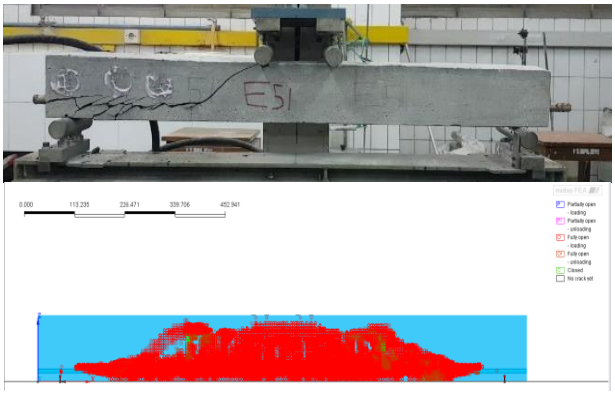

Fig. 9. Failure and Cracking Pattern of Beam E31

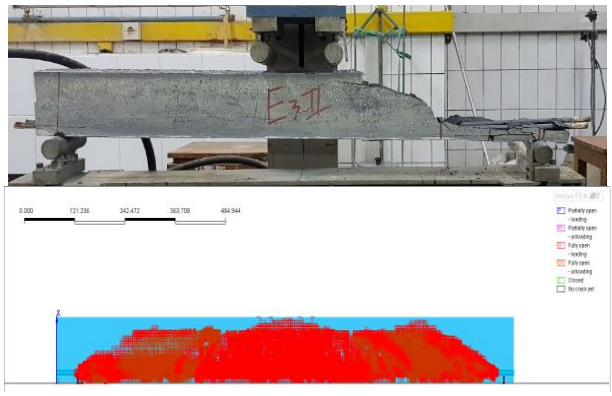

Fig. 10. Failure and Cracking Pattern of Beam E32

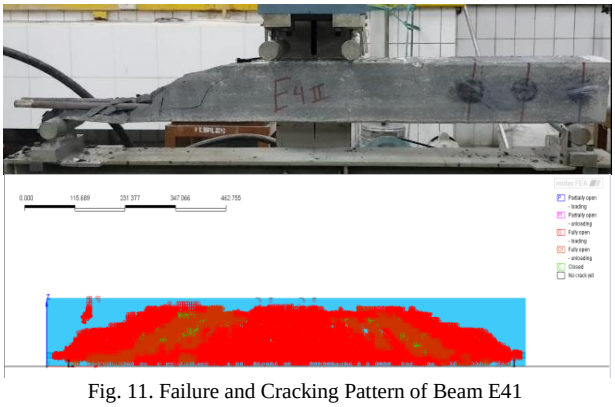

Fig. 11. Failure and Cracking Pattern of Beam E41

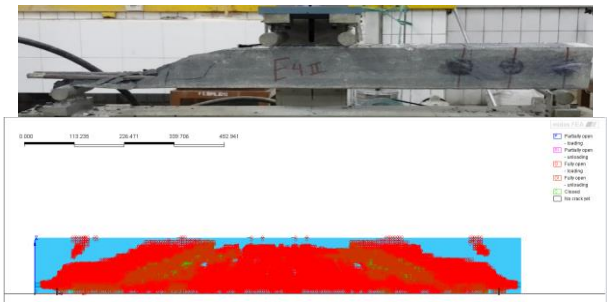

Fig. 12. Failure and Cracking Pattern of Beam E42

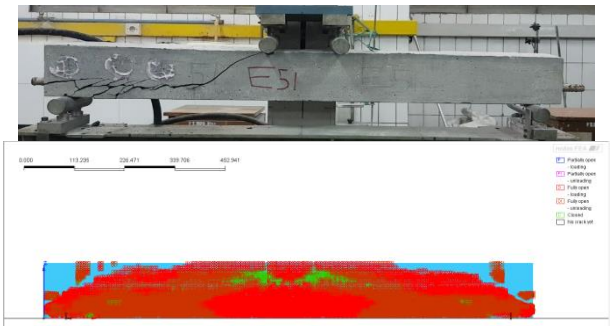

Fig. 13. Failure and Cracking Pattern of Beam E51

Fig. 14. Failure and Cracking Pattern of Beam E52

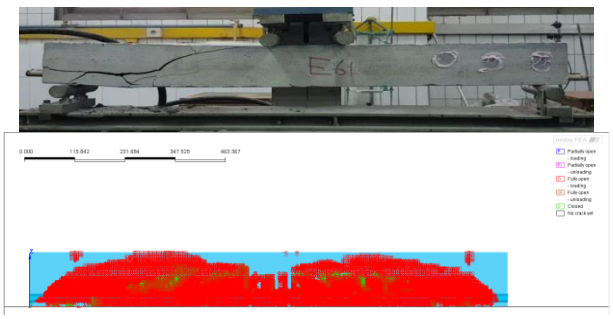

Fig. 15. Failure and Cracking Pattern of Beam E61

Fig. 16. Failure and Cracking Pattern of Beam E62

For beams E11 and E12, the cracks are first formed in the middle of the beam, and the cracks are generally vertical. This indicates flexural failure of the beam. By increasing the longitudinal reinforcement ratio from 0.73% to 1.32%, the inclined cracks associated with shear failure can also be observed along with the vertical cracks. For beams E31 to E62, diagonal cracks from the location of concentrated load to the nearest support can be seen from the test results and the MIDAS FEA output.

The maximum loads at failure obtained from MIDAS FEA are tabulated in Table V. The maximum loads that can be carried by the beams based on its theoretical bending capacity (P_M) and its theoretical shear capacity (P_V) are also tabulated in Table V. The maximum loads from experiment and finite element analysis are shown in Fig. 17. The curved line in Fig. 17 represents the minimum value of P_M and P_V.

TABLE V
COMPARISON OF MAXIMUM LOAD

Beam ID	ρ (%)	P_{TEST} (kN)	P_{FEA} (kN)	P_{TEST} / P_{FEA}	P_M (kN)	P_V (kN)
E11	0.73	15.12	13.03	1.16	9.4	17.3
E12	0.73	14.73	14.28	1.03	9.4	17.6
E21	1.32	16.06	15.38	1.04	16.2	19.0
E22	1.32	17.37	15.32	1.13	16.2	18.4
E31	2.08	17.31	17.47	0.99	24.2	20.1
E32	2.08	23.13	18.34	1.26	24.6	22.6
E41	3.02	21.05	23.29	0.90	34.3	26.0
E42	3.02	23.81	24.03	0.99	33.5	23.3
E51	5.47	29.73	32.79	0.91	55.4	31.2
E52	5.47	29.94	33.40	0.90	55.6	31.6
E61	7.82	29.11	32.97	0.88	72.4	36.0
E62	7.82	27.70	37.76	0.73	70.3	34.2

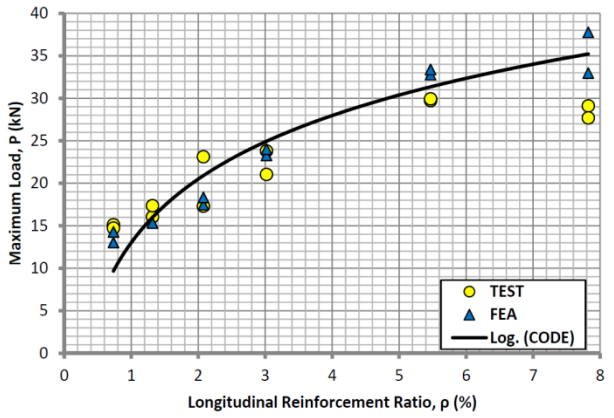

Fig. 17. Maximum Load vs Longitudinal Reinforcement Ratio

From Table V and Fig. 17, it can be seen that the finite element analysis results are quite close to the experiment results, especially at a longitudinal reinforcement ratio lower than 2%. As the longitudinal reinforcement ratio increases, the maximum load from finite element analysis becomes more overestimating the maximum load from the experiment. The overestimation, indicated by $P_{TEST}/P_{FEA} < 1$, can be seen from a longitudinal reinforcement ratio of about 3%. The lowest ratio of P_{TEST}/P_{FEA} of 0.73 ($P_{FEA} = 1.36P_{TEST}$) has been obtained from beam E62 with ρ = 7.82%. Because the longitudinal reinforcement ratio in the practical beam is usually less than 2% to 3%, the bond-slip modeling in this research gives an accurate estimation of SFRC beam failure and the maximum load at failure.

In order to eliminate the effect of variable concrete strength, a non-dimensional parameter called normalized shear stress (v_{norm}) is determined. In this research, the maximum limit of ACI 318-19 concrete shear strength will only govern for very high values of ρ. Thus, by rearranging Eq. (4), v_{norm} can be defined as

$$v_{norm} = \frac{V_c}{bd(f'_c)^{1/2}} = C_1(\rho)^{C_2} \quad (5)$$

where C_1 = 0.66 and C_2 = 1/3 in ACI 318-19. By taking logarithm values of both sides in Eq. (5), the following is obtained

$$\log(v_{norm}) = \log(C_1) + C_2 \log(\rho) \quad (6)$$

Coefficient C_1 and C_2 can be determined by linear regression as shown in Table VI, Table VII, and Fig. 18.

In this research, two sets of regression analyses are performed for two ranges of longitudinal reinforcement ratio, that is 0.73% to 7.82% and 0.73% to 3.02%. The results are presented in Table VII. It can be seen that the SFRC shear strength predicted by FEA is similar for the two ranges considered in this research.

TABLE VI
DETERMINATION OF NORMALIZED SHEAR STRESS FUNCTION

Beam ID	$\log(\rho)$	v_{norm} (Test)	v_{norm} (FEA)	$\log(v_{norm})$ (Test)	$\log(v_{norm})$ (FEA)
E11	–2.13	0.112	0.097	–0.95	–1.01
E12	–2.13	0.108	0.105	–0.97	–0.98
E21	–1.88	0.132	0.126	–0.88	–0.90
E22	–1.88	0.147	0.130	–0.83	–0.89
E31	–1.68	0.157	0.158	–0.81	–0.80
E32	–1.68	0.185	0.147	–0.73	–0.83
E41	–1.52	0.167	0.184	–0.78	–0.73
E42	–1.52	0.210	0.212	–0.68	–0.67
E51	–1.26	0.239	0.263	–0.62	–0.58
E52	–1.26	0.238	0.265	–0.62	–0.58
E61	–1.11	0.228	0.258	–0.64	–0.59
E62	–1.11	0.229	0.312	–0.64	–0.51

TABLE VII
NORMALIZED SHEAR STRESS FUNCTION

ρ (%)	Type	$\log(C_1)$	C_1	C_2	Function
0.73 to 7.82	ACI	–0.181	0.66	0.333	$v_{norm} = 0.66\,\rho^{0.333}$
	TEST	–0.237	0.58	0.329	$v_{norm} = 0.58\,\rho^{0.329}$
	FEA	–0.018	0.96	0.462	$v_{norm} = 0.96\,\rho^{0.462}$
0.73 to 3.02	ACI	–0.181	0.66	0.333	$v_{norm} = 0.66\,\rho^{0.333}$
	TEST	–0.133	0.74	0.385	$v_{norm} = 0.74\,\rho^{0.385}$
	FEA	–0.018	0.96	0.463	$v_{norm} = 0.96\,\rho^{0.463}$

From Table VII, the regression analysis of FEA results shows that the exponent factor (C_2) for SFRC beams is greater than C_2 for normal-weight concrete beams. It means that dowel action has a lesser influence on the shear strength of SFRC compared to normal-weight concrete. A lower influence of ρ on SFRC shear strength also can be observed from test results for a 0.73% to 3.02% reinforcement ratio. This trend is in accordance with previous research [14] for concrete without coarse aggregate.

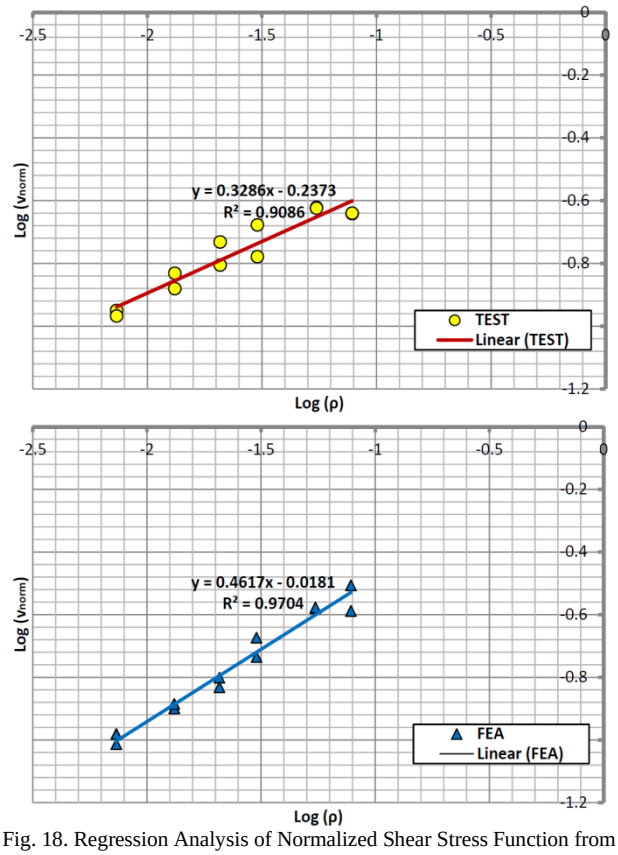

Fig. 18. Regression Analysis of Normalized Shear Stress Function from Test Results and Finite Element Analysis

IV. Conclusion

The shear strength of steel-fiber reinforced concrete beams without coarse aggregate can be predicted accurately for $\rho < 3\%$. By using only 18% of bond stress in the simplified bond stress-slip function for high-strength concrete, proposed by fib [27], the finite element analysis of the SFRC beams without coarse aggregate gives a similar cracking pattern and maximum load at failure, particularly at $\rho < 3\%$. For $\rho > 3\%$, both ACI 318-19 and the finite element model used in this research start to give overestimated value. The lowest ratio of the experiment's maximum load to the finite element's maximum load of 73% has been obtained for $\rho = 7.82\%$.

The influence of the longitudinal reinforcement ratio on the shear strength of SFRC beams without coarse aggregate is lower than the shear strength of normal-weight concrete predicted by ACI 318-19. The shear stress function for SFRC without coarse aggregate in this research can be expressed in the form of $V = 0.96\rho^{0.462}(f'_c)^{0.5}bd$.

For future research, the bond stress-slip relationship in SFRC beams without coarse aggregate needs to be investigated. The development of a simplified bond-slip function obtained from the experiment is needed for further studies. The effect of bar geometry (deformed or plain bar) on bonds in SFRC beams without coarse aggregate also needs to be investigated.

Acknowledgments

The authors would like to thank all the contributors to the research and those who have provided assistance and support during the experimental work in the Laboratory of Construction Material Technology, Department of Civil Engineering, Universitas Tarumanagara, Jakarta. Special thanks due to all sponsors, i.e. PT. Midasindo Teknik Utama for the Midas FEA, PT. Indocement Tunggal Prakarsa for the ordinary portland cement, and also PT. BASF for the superplasticizer and silica fume.

References

[1] D. Christianto, Tavio, D. Kurniadi, Effect of Steel Fiber on the Shear Strength of Reactive Powder Concrete, *IOP Conference Series: Materials Science and Engineering*, *Vol. 508*, 2019, pp. 1-10.

[2] M. Wulandari, M. F. Sofianto, Tavio, Split Tensile and Flexural Strength of Concrete with Artificial Lightweight Aggregate (ALWA) and Steel-Fiber, *Journal of Physics: Conference Series*, *IOP Publishing*, *Vol. 1569*, 2020, pp. 1-7.

[3] B. Sabariman, A. Soehardjono, Wisnumurti, A. Wibowo, Tavio, Stress-Strain Model for Confined Fiber-Reinforced Concrete under Axial Compression, *Archives of Civil Engineering*, *Vol. 66*, *No. 2*, 2020, pp. 119-133.

[4] M. M. Rafi, A. Nadjai, F. Ali, Analytical Modeling of Concrete Beams Reinforced with Carbon FRP Bars, *Journal of Composite Materials*, *Vol. 41*, 2007, pp. 2675-2690.

[5] B. Sabariman, A. Soehardjono, Wisnumurti, A. Wibowo, Tavio, Stress-Strain Behavior of Steel Fiber-Reinforced Concrete Cylinders Spirally Confined with Steel Bars, *Advances in Civil Engineering*, *Vol. 2018*, 2018, pp. 1-8.

[6] D. Pinto, Tavio, I G. P. Raka, Axial Compressive Behavior of Square Concrete Columns Retrofitted with GFRP Straps, *International Journal of Civil Engineering and Technology*, *Vol. 10*, *No. 1*, 2019, pp. 2388-2400.

[7] Tavio, M. Rafani, I G. P. Raka, V. Ratnasari, Flexural Capacity Predictions and Comparisons of GFRP Reinforced Beams, *Journal of Physics: Conference Series*, *IOP Publishing*, *Vol. 1477*, 2020, pp. 1-5.

[8] M. Rafani, A. Suhardjono, Wisnumurti, A. Wibowo, Tavio, A Theoretical Study of GFRP RC Beams Deflection, *Journal of Physics: Conference Series*, *IOP Publishing*, *Vol. 1477*, 2020, pp. 1-5.

[9] Y. Z. Murad, J. A. Zaid, Finite Element Modelling of Reinforced Concrete Beams Strengthened with Different Configuration of Carbon Fiber Sheets, *International Review of Civil Engineering (IRECE)*, *Vol. 10*, *No. 4*, 2019, pp. 188-196.

[10] Tavio, B. Kusuma, Stress-Strain Model for High-Strength Concrete Confined by Welded Wire Fabric," *Journal of Materials in Civil Engineering, ASCE*, *Vol. 21*, *No. 1*, 2009, pp. 40-45.

[11] H. Al-Quraishi, R. Abdulkhudhur, A. Abdulazeez, Shear Strength Behavior of Fiber Reinforced Recycled Aggregate Concrete Beams, *International Review of Civil Engineering (IRECE)*, *Vol. 12*, *No. 5*, 2021, pp. 314-322.

[12] A. Sandjaya, Tavio, D. Christianto, Experimental Study of Mortar Compressive Strength with Anadara Granosa Powder as a Substitute for Partial Use of Cement, *IOP Conference Series: Materials Science and Engineering*, *Vol. 650*, 2019, pp. 1-6.

[13] D. Christianto, C. A. Makarim, Tavio, Influence of Longitudinal Reinforcement Ratio on Shear Capacity of No Coarse-Aggregate Concrete, *International Journal of GEOMATE*, *Vol. 21*, *No. 86*, 2021, pp. 122-130.

[14] D. Christianto, Tavio, C. A. Makarim, Effect of Longitudinal Steel Reinforcement on Shear Capacity of SFRC Beams without Coarse Aggregate, *Technology Report of Kansai University*, *Vol. 63*, *No. 1*, 2021, pp. 6909-6917.

[15] D. Christianto, C. A. Makarim, Tavio, I. D. Pratama, Modified EC2's Shear Strength Equation for No Coarse Aggregate RC Beams, *International Journal on Advance Science Engineering*

Information Technology (IJASEIT), Vol. 12, No. 6, 2022, pp. 2211-2216.
[16] W. Widjaja, D. Christianto, D. Kurniadi, L. Monica, Yuliana, Michelle, Shear Capacity of Fiber-Reinforced Concrete Beams without Transverse Reinforcement, *IOP Conference Series: Materials Science and Engineering, Vol. 650*, 2019, pp. 1-12.
[17] D. Christianto, C. A. Makarim, Tavio, Y. U. Liucius, Size Effect on Shear Stress of Concrete Beam without Coarse Aggregate, *Journal of Physics: Conference Series, Vol. 1477*, 2020, pp. 1-7.
[18] D. Christianto, C. A. Makarim, Tavio, A. H. Jusuf, A Proposed Formula for Predicting Size Effect on Shear Strength of Concrete Beams without Coarse Aggregate, *International Journal on Engineering Applications (IREA), Vol. 10, No. 3*, 2022, pp. 220-226.
[19] Tavio, S. P. Machmoed, I G. P. Raka, Behavior of Square RC Columns Confined with Interlocking Square Spiral Under Axial Compressive Loading, *International Journal on Engineering Applications (IREA), Vol. 10, No.. 5*, 2022, pp. 322-335.
[20] D. Christianto, V. Marcella, C. Saka, A. N. Tanika, Y. Lase, Analysis of the Sand Grains Influence on Damping Ratio Using Shear Test, *Lecture Notes in Civil Engineering, Vol. 216, No. 1*, 2022, pp. 247-253.
[21] N. Rizqyani, Tavio, Proposed Formula and Comparison of Shear Strengths of Reinforced Concrete Beams under Various Codes, *International Journal of GEOMATE, Vol. 23, No. 99*, 2022, pp. 9-16.
[22] Joint ACI-ASCE Committee 445, *Recent Approach to Shear Strength of Structural Concrete (ACI 445R-99)* (American Concrete Institute, 1999).
[23] MIDAS FEA, *Analysis and Algorithm* (Midas IT Co., Ltd, 2016).
[24] J. K. Wight, *Reinforced Concrete: Mechanics and Design* (Pearson Education, Inc., 2016).
[25] L. Jendele, J. Cervenka, Finite Element Modeling of Reinforcement with Bond, *Computers and Structures, Vol. 84, No. 28*, 2006, pp. 1780-1791.
[26] ACI Committee 408, *Bond and Development of Straight Reinforcing Bars in Tension (ACI 408R-03)* (American Concrete Institute, 2003).
[27] fib, *Bond of Reinforcement in Concrete (Bulletin 10)* (International Federation for Structural Concrete, 2000).
[28] fib, *Structural Concrete: Textbook on Behaviour, Design, and Performance Updated Knowledge of the CEB/FIP Model Code 1990 Volume 1 (Bulletin 1)* (International Federation for Structural Concrete, 2000).
[29] G. Xing, C. Zhou, T. Wu, B. Liu, Experimental Study on Bond Behavior between Plain Reinforcing Bars and Concrete, *Advances in Materials Science and Engineering, Vol. 2015*, 2015, pp. 1-9.
[30] ACI Committee 318, *Building Code Requirements for Structural Concrete (ACI 318-19) and Commentary (ACI 318R-19)* (American Concrete Institute, 2019).

Authors' information

[1]Department of Civil Engineering, Universitas Tarumanagara, Jakarta, Indonesia.

D. Christianto is a doctoral candidate at the Department of Civil Engineering, Universitas Tarumanaraga, Jakarta, Indonesia. He is also a lecturer at the same university as he is currently pursuing his doctoral degree. His research interest includes concrete materials and structural members, particularly in high-strength concrete and reactive powder concrete.

[2]Department of Civil Engineering, Institut Teknologi Sepuluh Nopember (ITS), Surabaya, Indonesia. *Corresponding author.

Tavio is a professor at the Department of Civil Engineering, Institut Teknologi Sepuluh Nopember (ITS), Surabaya, Indonesia. His research interest includes forensic and retrofitting in civil engineering, analytical/numerical and experimental modeling for simulating the behavior and performance of reinforced and prestressed/precast concrete members including composite and steel structures under seismic loading and fire conditions, concrete, steel and rubber materials for structural use, dampers and isolation systems for seismic mitigation.

[3]Department of Civil Engineering, Universitas Tarumanagara, Jakarta, Indonesia.

M. R. Irianto iss an undergraduate student in the Department of Civil Engineering, Universitas Tarumanagara, Jakarta, Indonesia. His final project is about bond-slip modeling for concrete beams.